doi:10.1111/j.1558-5646.2007.00071.x

THE MUTATION MATRIX AND THE EVOLUTION OF EVOLVABILITY

Adam G. Jones,[1,2] Stevan J. Arnold,[3] and Reinhard Bürger[4]

[1]*Department of Biology, 3258 TAMU, Texas A&M University, College Station, Texas 77843*

[2]*E-mail: agjones@tamu.edu*

[3]*Department of Zoology, 3029 Cordley Hall, Oregon State University, Corvallis, Oregon 97331*

[4]*Institut für Mathematik, Universität Wien, Nordbergstrasse 15, 1090 Wien, Austria*

Received June 12, 2006
Accepted December 7, 2006

Evolvability is a key characteristic of any evolving system, and the concept of evolvability serves as a unifying theme in a wide range of disciplines related to evolutionary theory. The field of quantitative genetics provides a framework for the exploration of evolvability with the promise to produce insights of global importance. With respect to the quantitative genetics of biological systems, the parameters most relevant to evolvability are the G-matrix, which describes the standing additive genetic variances and covariances for a suite of traits, and the M-matrix, which describes the effects of new mutations on genetic variances and covariances. A population's immediate response to selection is governed by the G-matrix. However, evolvability is also concerned with the ability of mutational processes to produce adaptive variants, and consequently the M-matrix is a crucial quantitative genetic parameter. Here, we explore the evolution of evolvability by using analytical theory and simulation-based models to examine the evolution of the mutational correlation, r_μ, the key parameter determining the nature of genetic constraints imposed by M. The model uses a diploid, sexually reproducing population of finite size experiencing stabilizing selection on a two-trait phenotype. We assume that the mutational correlation is a third quantitative trait determined by multiple additive loci. An individual's value of the mutational correlation trait determines the correlation between pleiotropic effects of new alleles when they arise in that individual. Our results show that the mutational correlation, despite the fact that it is not involved directly in the specification of an individual's fitness, does evolve in response to selection on the bivariate phenotype. The mutational variance exhibits a weak tendency to evolve to produce alignment of the M-matrix with the adaptive landscape, but is prone to erratic fluctuations as a consequence of genetic drift. The interpretation of this result is that the evolvability of the population is capable of a response to selection, and whether this response results in an increase or decrease in evolvability depends on the way in which the bivariate phenotypic optimum is expected to move. Interestingly, both analytical and simulation results show that the mutational correlation experiences disruptive selection, with local fitness maxima at –1 and +1. Genetic drift counteracts the tendency for the mutational correlation to persist at these extreme values, however. Our results also show that an evolving M-matrix tends to increase stability of the G-matrix under most circumstances. Previous studies of G-matrix stability, which assume nonevolving M-matrices, consequently may overestimate the level of instability of G relative to what might be expected in natural systems. Overall, our results indicate that evolvability can evolve in natural systems in a way that tends to result in alignment of the G-matrix, the M-matrix, and the adaptive landscape, and that such evolution tends to stabilize the G-matrix over evolutionary time.

KEY WORDS: **Adaptive landscape, genetic correlation, G-matrix, mutation, quantitative genetics, response to selection.**

© 2007 The Author(s). Journal compilation © 2007 The Society for the Study of Evolution.

The idea of evolvability and its evolution has assumed various guises (Dawkins 1989; Cheverud 1996; Wagner and Altenberg 1996; Kirschner and Gerhart 1998; Radman et al. 1999; Hansen and Houle 2004). Evolvability can profitably be viewed as the intrinsic capacity of a genome to produce adaptive variants (Wagner and Altenberg 1996). In quantitative genetics, the concept of evolvability is closely related to the variability and standing genetic variance of phenotypic traits. With respect to a single trait affected by many genes, evolvability is dependent upon the input of new genetic variance due to mutation each generation. For a phenotype comprising multiple quantitative traits, the relevant parameter is **M**, the mutational matrix, which describes the effects of new mutations on trait variances and covariances. For a response to selection to occur, the variance due to new mutations must be translated into standing genetic variance and covariance in the population by various microevolutionary processes. The population-level additive genetic variance is described by the **G**-matrix, which has additive genetic variances on its main diagonal and additive genetic covariances elsewhere (Lande 1979; Lynch and Walsh 1998). The additive genetic covariances reflect coupling between traits that arises from pleiotropy and linkage disequilibrium. The population's greatest capacity to evolve in trait space is along the first principal component of the **G**-matrix, also known as the genetic line of least resistance (Schluter 1996). In other words, the **G**-matrix is the proximate parameter most relevant to quantitative measures of evolvability. To understand the evolution of evolvability from this standpoint, we need to understand the evolution of the **G**-matrix and its determinants, including the **M**-matrix.

At equilibrium, the **G**-matrix and hence the immediate capacity of a population to evolve can be viewed as a balance between the processes that affect genetic variation and covariation. In an infinite population at equilibrium, the input of genetic variation each generation due to mutation and recombination exactly offsets the pruning and reshaping that arises from stabilizing selection (Lande 1980). In a more realistic view of the world, finite population size imposes erratic fluctuations on top of this simple deterministic picture, causing the cloud of genetic values described by the **G**-matrix to pulsate and wobble from generation to generation (Jones et al. 2003, 2004). Thus, the primary determinants of the **G**-matrix are selection (especially stabilizing selection), mutation, recombination, and finite population size. The extent to which these determinants change over time is the central issue in the evolution of evolvability.

In two previous reports we studied the evolution and stability of the **G**-matrix under various constant regimes of population size, mutation, and stabilizing selection (Jones et al. 2003, 2004). We resorted to computer simulation because analytical work and empirical studies have failed to define the conditions under which **G** is likely to be stable or unstable. One of our main findings was that different aspects of stability react differently to selection, mutation, and drift. In particular, we found that correlational selection, correlated pleiotropic mutational effects, and large population size promoted stability of the orientation of the **G**-matrix. In contrast, stability in the overall size and eccentricity of the **G**-matrix was increased only by population size (Jones et al. 2003). The addition of a moving optimum led to two important new insights (Jones et al. 2004). First, evolution along the genetic line of least resistance increased stability of the orientation of the **G**-matrix relative to stabilizing selection alone. Evolution across genetic lines of least resistance decreased **G**-matrix stability. Second, evolution in response to a continuously changing optimum for one trait can produce persistent maladaptation in a correlated trait, even if its optimum does not change. In those simulations, as in virtually all other theoretical work, we employed a constant, nonevolving pattern of pleiotropic mutation.

In this report we consider the possibility that the pattern of pleiotropic mutation might evolve in response to selection. Although many estimates exist for the mutational variance, which corresponds to the diagonal elements of **M,** of single traits (Lynch and Walsh 1998; Lynch et al. 1999), only a few studies have assessed the rate and pattern of pleiotropic mutation, that is, the off-diagonal elements of **M** (Lynch 1985; Houle et al. 1994; Fernández and López-Fanjul 1996; Camara and Pigliucci 1999; Keightley et al. 2000; Estes et al. 2005). Comparative studies of **M** are nonexistent. Theoretical studies have modeled the composition of the **M**-matrix, but very little work has addressed the question of whether and how it evolves (Hermisson et al. 2003; Liberman and Feldman 2005). Thus, one of our goals is to provide some theoretical expectations about **M**-matrix evolution that might guide experimental and comparative studies of pleiotropic mutation. The **M**-matrix is the most important genetic parameter affecting evolvability, so the extent to which **M** evolves and responds to selection will provide direct insights into the evolution of evolvability.

Our second goal is to determine how an evolving pattern of pleiotropic mutation might affect evolvability through its effects on the **G**-matrix, the quantitative genetic parameter most directly relevant to the response to selection. If, for example, the **M**-matrix evolves toward alignment with the adaptive landscape, such evolution would also promote evolutionary alignment of **G** with the landscape. The result would be coincidence in genetic and selective lines of least resistance (Arnold et al. 2001). Alternatively, **M** might be a genetic constraint that maintains its independence in the face of selection. Thus, if the **M**-matrix does not respond to selection, we can expect the genetic line of least resistance to be a compromise between the major axes of the **M**-matrix and the adaptive landscape.

Our third goal is to determine how an evolving pattern of pleiotropic mutation might affect the stability of the **G**-matrix.

Two extreme outcomes are conceivable. On the one hand, evolution of **M** that promotes alignment of **M** and **G** with the adaptive landscape might promote stability of the **G**-matrix. On the other hand, weak selection on pleiotropic mutation coupled with drift due to finite population size might make **M** prone to stochastic fluctuations that destabilize the **G**-matrix. One of our aims is to determine the conditions under which these and other outcomes might prevail. We address these issues by developing a two-trait, quantitative genetic model of **M** evolution in which the diagonal elements of the matrix are held constant, whereas the mutational correlation is assumed to be a quantitative trait determined by multiple additive loci. We use this model to explore the evolutionary dynamics of the mutational correlation under stabilizing selection, with a particular emphasis on the evolution of evolvability and the stability of the **G**-matrix.

Theoretical Background

To anticipate some of the simulation results it will be useful to review a few theoretical topics. First, we consider the proposition that the mutational matrix might evolve toward alignment with the adaptive landscape. Lande (1980) constructed a model for the additive genetic covariance of multiple traits affected by many genes in a genetic system with stabilizing selection, pleiotropic mutation, and an arbitrary pattern of recombination but no dominance or epistasis. From Lande's results, and assuming random mating, one can readily derive the following relation for the matrix describing the input of additive genetic variance and covariance each generation due to mutation in an infinite-sized population at equilibrium under multivariate stabilizing selection:

$$\zeta \boldsymbol{M} = -\boldsymbol{G} H G,$$

where ζ is the total mutation rate of the traits (Phillips and Arnold 1989; Arnold 1992). The right side of the equation represents the change in genetic variance and covariance within a generation due to stabilizing selection. **G** is the additive genetic variance–covariance matrix before selection and **H** is the matrix describing the curvature and orientation of the adaptive landscape, that is, $H_{ij} = \partial^2 \ln \bar{W} / \partial \bar{z}_i \partial \bar{z}_j$ (Lande 1979, 1980). **H** is equal to $\gamma - \beta\beta^T$, where γ and β are, respectively, vectors of estimable coefficients of stabilizing and directional selection (Lande and Arnold 1983; Phillips and Arnold 1989) and ^{T} denotes the transpose of the vector. Using theorems given by Flury (1988, pp. 56–60), one can show that if all three symmetric matrices are positive definite, and **M** and **H** have common principal components (all eigenvectors aligned), so will **G**. Indeed, if any two of the three matrices have common principal components, so will the third. Consequently, if **M** should evolve to a configuration in which its eigenvectors are aligned with those of the adaptive landscape (i.e., **M** and **H** have common principal components), the eigenvectors of **G** will be aligned with both **M** and **H**. Alternatively, if we anticipate that **G** and **H** have aligned eigenvectors under the argument of phenotypic integration (Olson and Miller 1958; Cheverud 1984), then we should also anticipate that **M** will be aligned with both of those matrices. Thus, the issue we wish to resolve by computer simulation is whether **M** (and hence **G**) will evolve toward alignment with the adaptive landscape. We next consider the magnitude of selection acting on the off-diagonal elements of **M**.

The key parameter in the evolution of a two-dimensional **M**-matrix, at least from the perspective of the present study, is the mutational correlation (or mutational covariance), because the mutational correlation plays a central role in producing evolutionary constraints (Jones et al. 2003, 2004). This mutational correlation describes the pattern of pleiotropic mutation for two traits. We treat the mutational correlation, r_μ, as a quantitative trait that is affected by many loci. If the two traits are under stabilizing selection, but r_μ itself does not experience direct selection, one might surmise that r_μ will be subject to weak, indirect selection. Results presented later bear out this supposition.

To derive expressions for selection on the mutational correlation we will need some basic results from quantitative genetics. Suppose that viability selection on the two traits z_1 and z_2 is produced according to a Gaussian individual selection surface, such that the probability of survival of phenotype **z**, $W(\mathbf{z})$, is given by

$$W(z) = \exp\{-\tfrac{1}{2}(\mathbf{z} - \boldsymbol{\theta})^{\mathrm{T}} \boldsymbol{\omega}^{-1} (z - \boldsymbol{\theta})\}, \qquad (1)$$

where the magnitude and pattern of stabilizing selection is described by the matrix ω, and θ is a column vector that denotes the trait optima. Selection on the mutational correlation trait is only indirect, that is, via this individual selection function on **z**. The selectional correlation is the standardized off-diagonal element of $\boldsymbol{\omega}$: $r_\omega = \omega_{12}/\sqrt{\omega_{11}\omega_{22}}$. Following Lande (1979, 1980), we assume that the column vector of phenotypic measurements of the trait is given by

$$z = g + e,$$

where the distributions of **z**, **g** (the vector of additive genetic values), and **e** (the vector of environmental contributions) are approximately multivariate Gaussian with positive definite covariance matrices **P**, **G**, and **E**. Genetic values **g** and environmental contributions **e** are assumed to be stochastically independent, that is, there is no genotype-environment interaction, and **e** is scaled such that **E** is the identity matrix. In particular, these stipulations ensure that

$$\boldsymbol{P} = G + E. \qquad (2)$$

The mean fitness of the population is calculated to be

$$\bar{W} = e^{-A}\sqrt{\left|\boldsymbol{P}^{-1}\right| / \left|\boldsymbol{P}^{-1} + \omega^{-1}\right|}, \quad (3)$$

where || denotes the determinant of the matrix,

$$A = \frac{1}{2}(\bar{\mathbf{z}} - \theta)^T \omega^{-1}(\mathbf{P}^{-1} + \omega^{-1})^{-1}\mathbf{P}^{-1}(\bar{\mathbf{z}} - \theta),$$

and $\bar{\mathbf{z}}$ is the mean phenotype (Lande 1979). This result requires only that the distribution of phenotypes is Gaussian. In a later section we will use this result in equation (3) to derive expressions for the magnitude of selection on the mutational correlation.

Methods

THE SIMULATION MODEL

The simulation-based model of multivariate evolution that we use is a modification of the model used by Jones et al. (2003, 2004). That basic multivariate model is in turn a direct extension of the univariate models employed by Bürger et al. (1989) and Bürger and Lande (1994). We use a Monte Carlo approach to simulate a population of diploid, sexually reproducing organisms with two quantitative phenotypic traits. The life cycle consists of (1) production of progeny, including mutation and recombination; (2) viability selection; and (3) random selection of N adults from the survivors of selection. The mating system is monogamous and each breeding pair produces exactly four offspring. We restrict attention to parameter values under which at least N of the $2N$ offspring survive viability selection. Our random selection of adults then culls the population to a total of N before the next round of reproduction. Under these circumstances, the effective population size is larger than the census population size. We use population sizes of 256, 512, 1024, and 2048, which correspond to effective population sizes of 342, 683, 1366, and 2731 (Bürger and Lande 1994; Jones et al. 2003, 2004).

To investigate the evolution of evolvability, we extend the models used by Jones et al. (2003, 2004) by adding a third trait, the mutational correlation, which allows the mutational matrix, **M**, to evolve as this trait changes. The mutational correlation, r_μ, describes the extent to which the mutational effects on two other traits, z_1 and z_2, are correlated. The mutational correlation itself is determined by n_r unlinked additive loci, which we model explicitly. Unless otherwise stated, we use $n_r = 10$. Thus, each individual has a personal value for the mutational correlation. Each generation we allow a mutation to occur at each of these loci at a rate of $\mu_r = 0.0002$. When a mutation occurs, we randomly draw a mutational effect from a Gaussian distribution, with a mean of zero and a variance of α_r^2, and add it to the existing values for the allele in question according to the continuum of alleles model (Crow and Kimura 1964). We transform the value of the mutational correlation to prevent it from taking values outside the range $(-1, 1)$. Let r_μ^* be the untransformed correlation and r_μ be the transformed value. Assuming that r_μ^* is the value of the trait after simply summing the effects of all 10 additive loci, the value of the mutational correlation, r_μ, which specifies the correlation between mutational effects at the pleiotropic loci determining the two phenotypic traits is given by

$$r_\mu = \frac{2e^{2r_\mu^*}}{1 + e^{2r_\mu^*}} - 1.$$

This transformation has the property that $r_\mu \approx r_\mu^*$ if $-0.5 < r_\mu^* < 0.5$ and r_μ converges to $+1$ or -1 as r_μ^* tends to $+\infty$ or $-\infty$. Because correlations take values between –1 and 1 by definition, some sort of transformation of the trait is necessary. The exact choice of transformation is arbitrary, but additional simulation runs (not shown) suggest that our results are robust to different methods of constraining the values of the mutational correlation.

We assume that the two phenotypic traits, z_1 and z_2, are determined by 50 unlinked pleiotropic loci. Mutations at these loci occur at a rate of $\mu = 0.0002$, and mutational effects, drawn randomly from a bivariate Gaussian distribution with a mean of 0 and variances of α_1^2 and α_2^2, are added to the existing values of the allele. The correlation of the mutational effects on the two traits is determined by the value of the mutational correlation for the individual in question. An individual's phenotype for z_1 and z_2 is determined by summing additive effects across loci and adding an environmental value drawn from a Gaussian distribution with a mean of zero and a variance of one. The environmental variance essentially defines the scale of the model. Hence, changes in the mutational variance, mutation rates, and the rate at which the optimum moves, for example, should be interpreted relative to the environmental variance. Our typical parameter values usually produce single-trait heritabilities near 0.2, a sufficiently high value to allow a strong response to selection. The loci that determine the mutational correlation are distinct from the loci that determine the phenotypic traits, so there is no inherent genetic mechanism that would produce a genetic correlation between the mutational correlation trait and the other two traits. Viability selection on the two traits z_1 and z_2 is produced according to a Gaussian individual selection surface, as described by equation (1). Selection on the mutational correlation trait is indirect via this individual selection function on z_1 and z_2. In other words, an individual's value of r_μ has no direct role in the calculation of that individual's fitness.

Each simulation run starts with an initially genetically uniform population that evolves for 10,000 generations under a regime of stabilizing selection. Additive genetic variance accumulates due to random mutation, and the population achieves a stabilizing selection-mutation-drift equilibrium. These 10,000 generations are followed by an additional 10,000 generations of experimental evolution during which we record quantitative

Table 1. Summary of variables and parameters used in the simulations.

Symbol	Definition
ω	Strength of stabilizing selection on z_1 and z_2.
r_ω	Selectional correlation.
r_μ	Mutational correlation.
μ	Per locus mutation rate for z_1 and z_2.
ζ	Total mutation rate of the traits ($\zeta = 2n\mu$).
μ_r	Per locus mutation rate for the mutational correlation, r_μ.
α_r^2	Per locus variance in mutational effects on r_μ.
α_1^2	Per locus variance in mutational effects on z_1.
α_2^2	Per locus variance in mutational effects on z_2.
G_{11}	Additive genetic variance for trait 1.
G_{22}	Additive genetic variance for trait 2.
G_{12}	Genetic covariance between traits 1 and 2.
r_g	Genetic correlation between traits 1 and 2.
λ_1	Leading eigenvalue, indicating the length of the long axis of the **G**-matrix.
λ_2	Second eigenvalue, indicating width of the **G**-matrix (i.e., orthogonal to φ).
Σ	The size of the **G**-matrix, ($\lambda_1 + \lambda_2$ or $G_{11} + G_{22}$).
ε	The eccentricity of **G** (λ_2/λ_1); smaller values indicate greater eccentricity.
ϕ	The angle of the leading eigenvector (i.e., the genetic line of least resistance).

genetic variables of interest. In this article, we only deal with the effects of stabilizing selection on the evolution of the mutational correlation. The directional selection case is interesting, but beyond the scope of the present analysis. Table 1 presents a summary of important parameters and variables used in the simulations.

CHARACTERIZING G-MATRIX STABILITY

The most obvious way of studying the degree of stability of the size and shape of the **G-**matrix is to consider the genetic variances of the two traits (G_{11}, G_{22}), their covariance (G_{12}), or correlation (r_g), and their temporal dynamics. An alternative is to look at the eigenvalues (λ_1, λ_2), their ratio ($\varepsilon = \lambda_2/\lambda_1$, a measure inversely related to the eccentricity), and the angle (φ) between the leading eigenvector and the axis along which the first trait is measured (i.e., the x-axis). This angle φ is measured in degrees and ranges from -90° to $+90^\circ$, thus providing a convenient measure for the orientation of the **G-**matrix. The total genetic variance, $\Sigma = G_{11}+G_{22}$, can be used as a measure of the overall size of the **G**-matrix. Thus, a two-dimensional **G**-matrix is fully described by Σ, ε, and φ. These ways of characterizing and visualizing **G**-matrices are discussed at greater length elsewhere (Jones et al. 2003, 2004).

Results

SELECTION ON THE MUTATIONAL CORRELATION: ANALYTICAL RESULTS

For the case of two characters, we now present two different kinds of approximations for the **G**-matrix, the mean fitness, and the directional selection gradient of the mutational correlation at pleiotropic mutation-selection balance. Therefore, we set $\bar{\mathbf{z}} = \boldsymbol{\theta}$ in what follows. This theory also assumes that the population is sufficiently large that random genetic drift can be ignored (an assumption that will be relaxed in the simulation-based study).

Lande's Gaussian theory

For additively determined traits, that is, in the absence of dominance and epistasis, Lande (1980) derived the following formula for the **G**-matrix at equilibrium under mutation-selection balance:

$$\mathbf{G} = 2\sum\nolimits_i \mathbf{V}_s^{1/2}\left(\mu_i \mathbf{V}_s^{-1/2}\mathbf{M}_i\mathbf{V}_s^{-1/2}\right)^{1/2}\mathbf{V}_s^{1/2}. \quad (4)$$

Here, the sum is over all n loci contributing to the trait, μ_i is the per-locus mutation rate, $\mathbf{M}_i$ is the **M**-matrix of locus i, and $\mathbf{V}_s = \boldsymbol{\omega} + \mathbf{E}$ is the matrix describing stabilizing selection on the genotypic values. The square roots of the matrices are taken to be positive (semi) definite. The derivation of equation (4) assumes linkage equilibrium and, essentially, that the distribution of allelic effects at each locus is multivariate Gaussian, which requires that the mutational variances, α_i^2, at each locus are much smaller than the per-locus standing genetic variances, G_{ii}.

For two characters, if stabilizing selection on both traits is equally strong ($\omega = \omega_{11} = \omega_{22}$) and the loci are mutationally equivalent (i.e., $\mu_i \equiv \mu$, $\mathbf{M}_i \equiv \mathbf{M}$ for $i = 1, 2$, and $\alpha^2 \equiv \alpha_1^2 = \alpha_2^2$), some simple and explicit results can be obtained. These assumptions imply that the eigenvectors of $\boldsymbol{\omega}$, $\mathbf{V}_s$, and **M** are all (1,1) and (1,−1) if the correlations do not vanish, and (1,0) and (0,1), otherwise. For a positive correlation, (1,1) is the leading eigenvector. For instance, the diagonal elements of **G** are calculated to be

$$G_{11} = G_{22} = \frac{1}{2}V_G\left(\sqrt{1+r_s}\sqrt{1+r_\mu} + \sqrt{1-r_s}\sqrt{1-r_\mu}\right), \quad (5)$$

where $r_s = \frac{\omega}{\omega+1}r_\omega$ is the "correlation" in the matrix $\mathbf{V}_s$, and

$$V_G = 2n\sqrt{\mu\alpha^2 V_s}, \quad (6)$$

is the so-called Gaussian approximation for the equilibrium genetic variance for a single trait ($V_S = \omega + 1$). The genetic covariance is

$$G_{12} = \frac{1}{2}V_G\left(\sqrt{1+r_s}\sqrt{1+r_\mu} - \sqrt{1-r_s}\sqrt{1-r_\mu}\right) \quad (7)$$

and for the genetic correlation, one obtains

$$r_g = \frac{1 + r_s r_\mu - \sqrt{1 - r_s^2}\sqrt{1 - r_\mu^2}}{r_s + r_\mu}. \quad (8)$$

We note that if $r_\mu = r_s$, then $r_g = r_\mu = r_s$.

By assuming that equations (6) and (7) are accurate approximations, an explicit but complicated expression for the mean fitness at equilibrium can be derived from equation (3). The following much simpler expression is obtained by neglecting terms of order $(V_G/V_S)^2$ and smaller:

$$\bar{W}_{Gau} = \frac{\sqrt{1 - r_\omega^2}}{\sqrt{v^2 - r_\omega^2}}\left[1 - \frac{V_G}{2V_S}\left(\frac{\sqrt{1 + r_\mu}}{\sqrt{1 + r_s}} + \frac{\sqrt{1 - r_\mu}}{\sqrt{1 - r_s}}\right)\right], \quad (9)$$

where $v = V_S/\omega$. For the directional selection gradient of r_μ we obtain, by assuming $v \approx 1$ and omitting terms of order $(V_G/V_S)^2$ and smaller, the approximation

$$\frac{\partial \ln \bar{W}_{Gau}}{\partial r_\mu} \approx \frac{V_G}{4V_S}\left(\frac{1}{\sqrt{1 - r_s}\sqrt{1 - r_\mu}} - \frac{1}{\sqrt{1 + r_s}\sqrt{1 + r_\mu}}\right). \quad (10)$$

This result shows that directional selection on the mutational correlation is, in general, weak and proportional to V_G/V_S. It is zero if, to the order of approximation considered here, $r_\mu = -r_\omega$, which corresponds to antialignment of the **M** and the $\mathbf{V}_s$ matrix.

The Zhang–Hill approximation

Recently, Zhang and Hill (2002) derived formulas for genetic variances and covariances under different assumptions. They also assumed linkage equilibrium and neglected random drift, but imposed conditions that are equivalent to the house-of-cards, or rare-allele, assumptions of Turelli (1984, 1985) and Barton and Turelli (1989). These conditions apply if per-locus mutation rates are sufficiently low or the variances of (per-locus) mutational effects, α_i^2, are larger than the standing (per-locus) variances, G_{ii} (Bürger 2000, Chap. 6). By the central limit theorem, the distribution of **g** can still be approximately normal, even if the single-locus distributions are not. This normality result only requires that sufficiently many loci contribute to the trait (and their effects do not vary too much). Zhang and Hill (2002) obtained results that generalize those of Turelli (1985) in several ways. If, as assumed in equations (5) through (8), loci are mutationally equivalent and stabilizing selection on both traits is equally strong, their result (A21) simplifies to

$$G_{11} = G_{22} = V_{HC}\frac{1 - r_s^2 + \sqrt{1 - r_s^2}\sqrt{1 - r_\mu^2}}{1 - r_s r_\mu + \sqrt{1 - r_s^2}\sqrt{1 - r_\mu^2}}, \quad (11)$$

where the so-called house-of-cards approximation to the genetic variance in mutation-selection balance for a single trait (Turelli 1984; Bürger 2000) is

$$V_{HC} = 2\zeta V_s, \quad (12)$$

with the total mutation rate of the trait $\zeta = 2n\mu$.

The genetic variances G_{ii} in equation (11) depend on r_μ and r_s in a qualitatively different way than they do in the Gaussian approximation in equation (5). Interestingly, however, the genetic correlation (equation (13) in Zhang and Hill (2002)) can be shown to be equal to equation (7) in the present symmetric case. In fact, the genetic correlations predicted by both models are always identical (Krall 2005). This result is somewhat unexpected but can be observed from Turelli's (1985) numerical computations.

For the mean fitness at equilibrium, we obtain from equation (3), by using equations (2), (11), and (7), the accurate approximation

$$\bar{W}_{ZH} = W_0\left[1 - 2\zeta + 4\zeta^2\left(1 + \frac{\left(1 - r_s r_\mu - \sqrt{1 - r_s^2}\sqrt{1 - r_\mu^2}\right)^2}{2(r_s - r_\mu)^2}\right)\right], \quad (13)$$

where terms of order ζ^3 and smaller have been neglected. Here, fitness of a genetically monomorphic population with $\bar{\mathbf{z}}$ at the optimum, and fitness deviation from one caused solely by environmental effects, is

$$W_0 = \frac{\sqrt{(V_s - 1)^2 - r_s^2 V_s^2}}{V_s\sqrt{1 - r_s^2}} \approx 1 - \frac{1}{V_s(1 - r_s^2)},$$

where the approximation is accurate if V_s is large. In equation (13), the dependence of mean fitness on r_μ is much weaker than under the Gaussian approximation because it is proportional to ζ^2. If $r_\mu \approx r_s$, the term by which $4\zeta^2$ is multiplied can be approximated by $1 + \frac{(r_s - r_\mu)^2}{8(1 - r_s^2)^2}$. Finally, the following approximation for the directional selection gradient of r_μ is readily derived (using *Mathematica*)

$$\frac{\partial \ln \bar{W}_{ZH}}{\partial r_\mu} \approx \frac{4W_0\zeta^2}{(r_s - r_\mu)^3}\cdot \left(2(1 - r_s^2)(1 - r_s r_\mu) - \frac{\sqrt{1 - r_s^2}}{\sqrt{1 - r_\mu^2}}\left[(1 - r_s r_\mu)^2 + (1 - r_s^2)(1 - r_\mu^2)\right]\right). \quad (14)$$

It is straightforward to show that the selection gradient is positive if and only if $r_\mu > r_s$. If $r_\mu \approx r_s$, equation (14) can be approximated by $W_0\zeta^2\frac{r_\mu - r_s}{(1 - r_s^2)^2}$.

Therefore, both approximations show that the mutational correlation is under disruptive selection. However, in contrast to the Gaussian prediction equation (10), under the Zhang–Hill approximation the selection gradient vanishes if $r_\mu = r_s$, is positive if $r_\mu > r_s$, and negative otherwise. The qualitatively different dependence of the selection gradient of r_μ in the Gaussian and the

Zhang–Hill approximation derives from the qualitatively different dependence of the genetic variances on r_μ. For the parameter ranges that are considered most plausible, the selection gradient under the Zhang–Hill approximation is much smaller than under Gaussian approximation because it is proportional to ζ^2.

The preceding expression in equation (14) for selection on r_μ assumed that the population mean was at the optimum. However, the mean of a finite population inevitably drifts around the optimum. As the mean phenotype is displaced from the optimum, the selection gradient varies because mean fitness changes even if the phenotypic covariance matrix remains constant. An explicit expression for the selection gradient under these conditions is obtained under the Zhang–Hill approximation by differentiating equation (3) and assuming that the genetic and phenotypic covariance matrices are unchanged as the mean phenotype drifts around the optimum. To leading order in ζ, we obtain

$$\frac{\partial \ln \bar{W}_{ZH}}{\partial r_\mu} \approx \frac{\zeta\,|\bar{\mathbf{z}}|^2}{\mathbf{V_S}} \frac{\sin(2\varphi) - r_s}{(r_s - r_\mu)^2} \left(\frac{1 - r_s r_\mu}{\sqrt{1 - r_s^2}\sqrt{1 - r_\mu^2}} - 1 \right), \tag{15}$$

where $(|\bar{\mathbf{z}}|, \varphi)$ denote the polar coordinates of the mean $\bar{\mathbf{z}}$, and the last term (in parentheses) is always nonnegative. Therefore, the selection gradient is maximized (and positive) if $\varphi = 45^\circ$ or $\varphi = -135^\circ$ (hence, the mean $\bar{\mathbf{z}}$ is a multiple of the leading eigenvector of $\mathbf{V}_s$), and minimized (and negative) if $\varphi = 135^\circ$ or $\varphi = -45^\circ$. If $r_\mu = r_s$, then equation (15) becomes $\frac{\zeta|\bar{\mathbf{z}}|^2}{\mathbf{V_S}} \frac{\sin(2\varphi) - r_s}{2(1-r_s)^2}$. Thus, if the mean phenotype is substantially displaced from the optimum, the selection gradient dramatically increases, because it becomes proportional to ζ. However, our numerical results discussed below show that excursions of more than 0.2 phenotypic standard deviations do not occur under the parameter combinations used in our simulations.

In the preceding analyses we assumed infinite population size. From our previous simulations (Jones et al. 2003, 2004), we expect finite population size will primarily affect the size of the **G**-matrix. No complete theory for the size of the **G**-matrix is available in the presence of random drift. However, because the size of the **G**-matrix is proportional to the genetic variance (of one of the traits), a reasonable approximation can be expected by replacing the single-trait genetic variance, V_G or V_{HC}, in any of the above formulas by its finite-population extension (see Bürger 2000, pp. 269–270). For the Zhang–Hill approximation, the house-of-cards variance in equation (12) has to be replaced by the so-called stochastic house-of-cards approximation

$$V_{SHC} = \frac{2\zeta V_s}{1 + V_s/(N_e \alpha^2)}, \tag{16}$$

where N_e denotes the effective population size. Figure 1 shows the genetic variance, the genetic correlation, and the mean fitness as a function of the mutational correlation for three different values of r_s. The left panels are from simulation, whereas the right panels are from the Zhang–Hill theory using equation (16) for the equilibrium genetic variance. The approximations are surprisingly good given that our theory neglects excursions of the mean from the optimum as well as nonconstancy of the **G**-matrix. The theory consistently overestimates the variance (as is known from the univariate case; Bürger 2000, Chap. 6), but the curves have approximately the correct shape.

One interesting result of this exercise is that the relationship between mean fitness and the value of the mutational correlation is, as noted above, qualitatively different for the Gaussian theory than it is for the Zhang–Hill approximation. Figure 2 shows a comparison of mean fitness as a function of the mutational correlation from the Zhang–Hill and Gaussian theory, with simulation results shown for comparison, when the selectional correlation (r_ω) is held constant at 0.75. As already noted, both approximations predict disruptive selection on r_μ, but it is striking that the positions of the fitness minima are contradictory. In addition, the difference between the maximum and minimum values of mean fitness differ by almost two orders of magnitude, indicating that selection on the mutational correlation is potentially much stronger in populations that satisfy the Gaussian assumptions than in those in which the Zhang–Hill theory apply. The simulation results appear to be intermediate, but perhaps closer to the Zhang–Hill assumptions. The Zhang–Hill assumptions are generally thought to be more realistic, a notion that stems in large part from results of quantitative trait locus mapping studies, which frequently find a few genes of major effect (Agrawal et al. 2001). These studies suggest that new mutations are large relative to the standing genetic variance, resulting in pattern that is more consistent with the Zhang–Hill than the Gaussian assumptions (Zhang and Hill 2002).

THE EVOLUTION OF THE MUTATIONAL CORRELATION

Our analytical results indicate that if the mean is very close to the optimum, the mutational correlation, r_μ, experiences only very weak, indirect selection, with selection gradients that, according to the Zhang–Hill approximation in equation (14), are proportional to ζ^2. Interestingly, r_μ is under disruptive selection. If the mean deviates from the optimum, which it usually does (slightly) due to random drift, the selection gradient becomes larger, and its sign depends on the position of the mean phenotype and on the selectional correlation (eq. 15). No simple prediction on the predominant direction of selection emerges in this case because the mean may evolve in a complex way. Because of this weak selection, the mutational correlation is prone to stochastic fluctuation arising from finite population size, and in many instances drift overwhelms response to selection (see below). Consequently, trends in response to selection were most apparent in large populations. Nevertheless, the mutational correlation does evolve, and

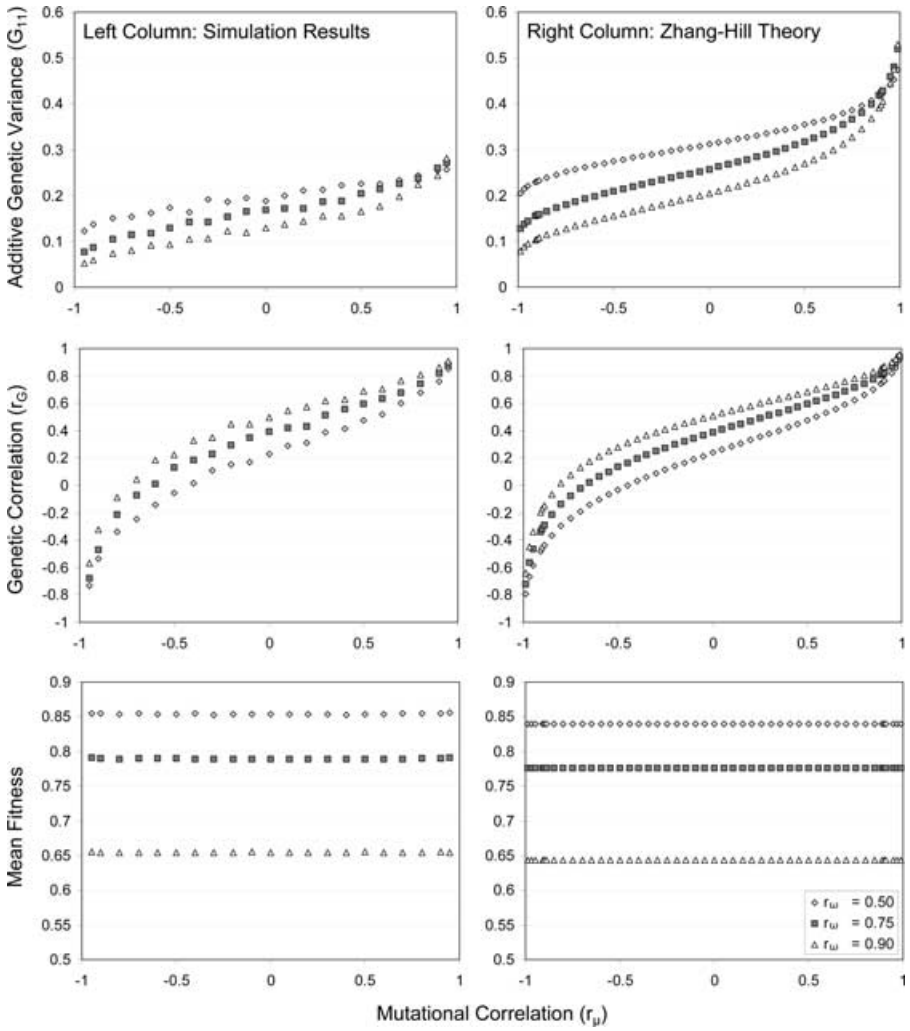

Figure 1. **The additive genetic variance of either phenotypic trait ($G_{11} = G_{22}$), the genetic correlation (r_g) between the two traits, and the mean fitness of the population as a function of the mutational correlation (r_μ). The panels on the left are generated from our simulation results and the panels on the right are based on the Zhang–Hill theory. The Gaussian model predicts exactly the same relationship between the genetic correlation and the mutational correlation as the Zhang–Hill theory. However, not shown here is the Gaussian model's predicted relationship between the mutational correlation and the additive genetic variance, which differs from that of the Zhang–Hill model in that it is maximized when $r_s = r_\mu$ (eq. 5). See Figure 2 for a comparison of mean population fitness as a function of r_μ under Gaussian versus Zhang–Hill assumptions. Parameter values are the same as those reported in Table 2.**

its evolution has a number of interesting consequences, which we report and discuss below.

As formulas in equations (10), (14), and (15) show, the mutational correlation can evolve in response to the shape of the adaptive landscape. The response to the selectional correlation r_ω is documented in Figure 3 and Table 2. Recall that in the results presented, the strength of stabilizing selection on both traits is equal ($\omega_{11} = \omega_{22}$). Hence, the eigenvectors of the adaptive landscape are always (1, 1) and (1, −1), unless $r_s = 0$. Even though results were extremely variable among runs, there is a clear tendency for stronger correlational selection to produce a mutational correlation of the same sign as the selectional correlation. Notice, however, in Table 2 and Figure 3 that alignment between mutation and selection is far from perfect. In particular, even when correlational selection is strong ($r_\omega = 0.9$), the average mutational correlation is only about 0.4 and in general $r_\mu < r_\omega$. Stochastic variation among replicate runs is responsible for this discrepancy. Thus, when $r_\omega = 0.9$, r_μ evolves to about 0.9 in a substantial fraction of runs, but in many other cases r_μ evolves to a much lower value, sometimes as low as −0.9 (Fig. 4). This indeterminacy in the evolution of r_μ can be expected from our expressions for the selection on r_μ which revealed an upward curvature of the adaptive landscape and hence an unstable equilibrium. In other words, the mutation matrix responds to selection imposed by the shape of the adaptive landscape but this trend is partially disguised by considerable indeterminacy in the evolution of r_μ.

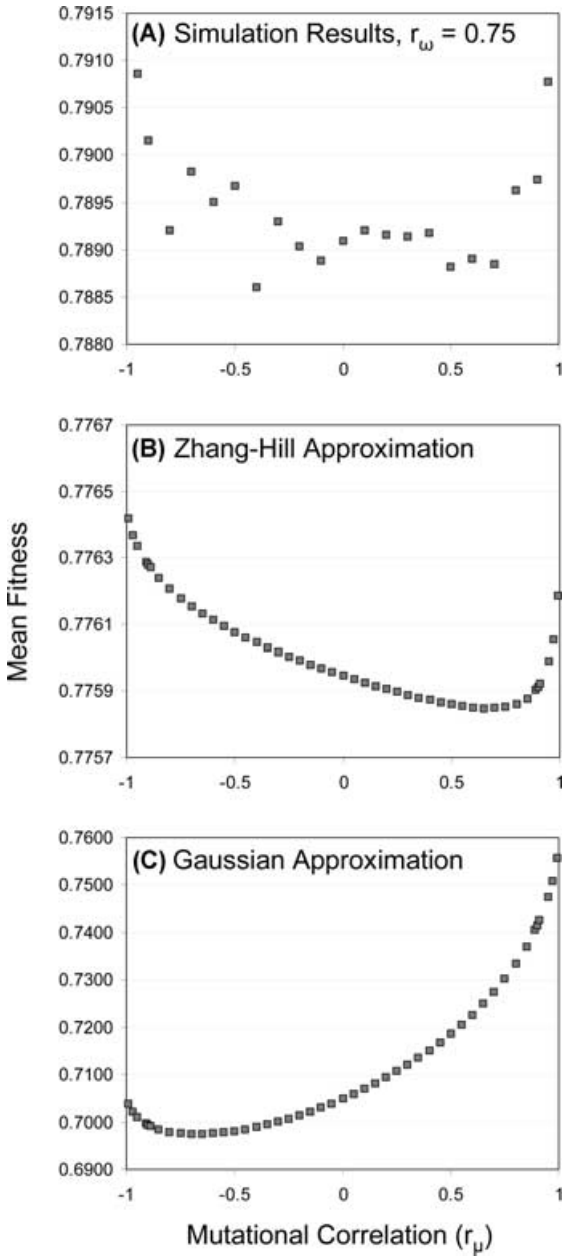

Figure 2. A closer look at the population mean fitness as a function of the mutational correlation from the simulation results (A), the Zhang–Hill theory (B), and the Gaussian theory (C). Parameter values are identical to those in Table 2. Note that each panel has a different scale. The value of the mutational correlation has a much stronger effect on mean fitness in the Gaussian case (C) than in the Zhang–Hill case (B). Each point in (A) represents mean population fitness across a total of 50,000 experimental generations from 10 independent runs (i.e., 5000 experimental generations preceded by 10,000 initial generations per run).

Does this pattern represent true alignment of the mutational matrix and the adaptive landscape? This question cannot be answered simply by altering the magnitude of correlational selection. As long as $\omega_{11} = \omega_{22}$, the angle of the adaptive landscape will be

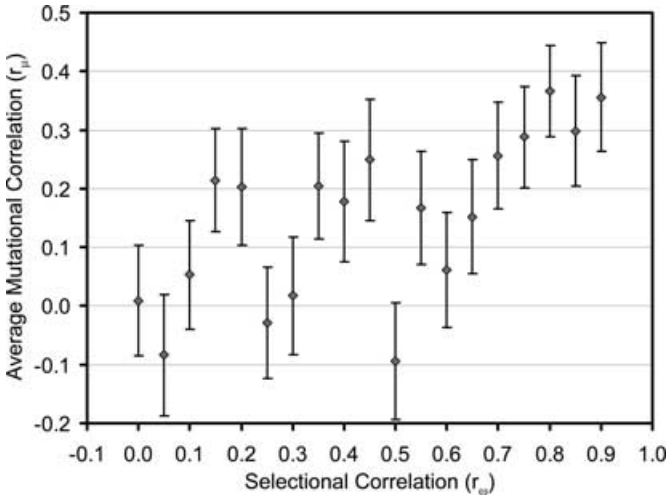

Figure 3. Evolution of the mutational correlation in response to selectional correlation of the adaptive landscape. Each symbol represents the mean population-level mutational correlation across 50 replicate simulation runs. The error bars show one standard error of the mean. These simulation runs were performed under the standard parameter set (see text and Table 2).

45° for positive r_ω and −45° for negative r_ω. However, changes in the ratio of ω_{11} to ω_{22} will produce variation in the angle of the adaptive landscape. In Figure 5, we examine the effects of such variation on the evolution of the mutational correlation by holding ω_{22} equal to 9 and varying ω_{11} from 9 to 64 in independent simulation runs. As the value of ω_{11} increases, the angle of the adaptive landscape decreases. If the mutational matrix is evolving toward alignment with the adaptive landscape, then we expect smaller values of the mutational correlation to evolve as the angle of the adaptive landscape decreases. Indeed, Figure 5 shows just such a pattern, implying that the mutational matrix does show a tendency to align itself with the adaptive landscape over evolutionary time.

On theoretical grounds we can expect the evolution of the mutational correlation to be enhanced by genetic variation in the correlation itself. The per-generation input of genetic variance in r_μ from mutation is proportional to the product of μ_r, α_r^2, and the number of loci affecting r_μ. Consequently, we can expect the evolution of r_μ to be enhanced by high values in any one of these parameters. Conversely, when the mutational correlation has almost no genetic variance (e.g., as a consequence of a small mutational variance), it should not respond to selection. As expected, higher mutational variance (α_r^2) of the mutational correlation results in the evolution of higher values of r_μ and the effect seems to be mediated by larger genetic variance in r_μ (Fig. 6). Similarly, as predicted by equation (14), the evolution of the mutational correlation is also enhanced by the mutability of the traits under direct selection, that is, by high mutation rates, μ_i, and large variances of mutational effects, α_i^2. As Figure 7 shows, the magnitude of the response of r_μ increases rapidly with α_i^2.

Table 2. The influence of the orientation of the adaptive landscape on the G-matrix when the mutational correlation is allowed to evolve versus when it is fixed.

r_ω	r_μ	G_{11}	G_{22}	G_{12}	r_g	λ_1	λ_2	Σ	ε	φ
Evolving r_μ										
−.90	−.30	.190	.190	−.148	−.557	.346	.034	.380	.204	−30.4
−.75	−.12	.182	.184	−.105	−.346	.310	.056	.366	.278	−21.2
−.50	.04	.189	.188	−.051	−.102	.304	.074	.377	.298	−7.0
.00	.02	.202	.201	.002	.001	.318	.085	.403	.308	1.5
.50	.12	.198	.197	.080	.234	.329	.067	.396	.255	14.0
.75	.34	.208	.206	.143	.521	.364	.050	.414	.224	29.1
.90	.40	.200	.201	.161	.590	.371	.030	.401	.143	31.9
Fixed r_μ										
−.90	.00	.130	.130	−.066	−.502	.197	.063	.260	.331	−45.1
−.75	.00	.163	.163	−.063	−.384	.228	.098	.326	.441	−45.2
−.50	.00	.196	.197	−.046	−.233	.247	.146	.393	.604	−44.8
.00	.00	.219	.219	.001	.003	.245	.192	.438	.789	.7
.50	.00	.197	.201	.047	.234	.250	.148	.398	.604	45.5
.75	.00	.163	.164	.064	.386	.229	.098	.326	.439	45.2
.90	.00	.132	.130	.067	.504	.199	.063	.262	.329	44.6
−.90	.50	.097	.097	−.025	−.247	.124	.070	.194	.588	−43.1
−.75	.50	.128	.129	−.014	−.105	.150	.107	.256	.727	−28.9
−.50	.50	.170	.171	.008	.049	.194	.148	.342	.767	16.5
.00	.50	.220	.220	.060	.275	.284	.156	.440	.557	44.9
.50	.50	.223	.222	.106	.475	.330	.115	.445	.354	44.9
.75	.50	.199	.198	.117	.589	.317	.080	.397	.258	44.8
.90	.50	.173	.173	.118	.681	.292	.054	.346	.190	45.1

Note: For these runs, we assumed a stationary optimum and the following parameter values: $N_e = 1366$, $\alpha_1^2 = \alpha_2^2 = \alpha_r^2 = 0.05$, $\omega_{11} = \omega_{22} = 9$, $n = 50$, $n_r = 10$, $\mu = \mu_r = .0002$. See text for other parameter values and for the definitions of these symbols. The top seven rows of values show results for an evolving r_μ, so the values for r_μ are means. In the lower section of the table, we fixed r_μ at either 0 or .5. The genetic values presented in this table are means, first averaged across the 10,000 "experimental" generations within a run and then averaged across 50 independent simulation runs for each parameter combination. The 10,000 experimental generations were preceded by 10,000 generations during which the population was allowed to accumulate genetic variation and reach quasiequilibrium. Standard errors are typically much smaller than the means, except for values of r_μ (see Figure 3), φ, and those very close to zero (e.g., .001 and .002). The standard errors for G_{11}, for instance, are between .001 and .012.

If the evolution of the mutational correlation is governed by the interplay of drift and selection, then an increase in population size should result in a more obvious response to selection. There does appear to be a trend for larger populations to respond more strongly to correlational selection relative to smaller populations (Fig. 8). The effect is most noticeable for very strong selectional correlations. For example, under a selectional correlation of 0.9, a population with an effective size of 2731 shows a mean mutational correlation greater than 0.5, whereas smaller populations show progressively smaller values (Fig. 8). Nevertheless, drift appears to be important even in the large population, as can be inferred from the extremely large standard errors (Fig. 8).

THE EVOLUTION OF THE G-MATRIX

The evolution of the mutational correlation contributes to the evolution of the **G**-matrix. Because the mutational correlation evolves, on average, to positive values if the selectional correlation is positive (and to negative values if the selectional correlation is negative), the same is true for the genetic correlation (Fig. 1 and Table 2). Notice that the angle of the **G**-matrix (φ) usually evolves toward alignment with the adaptive landscape even when r_μ is fixed at zero or 0.5. When r_μ is allowed to evolve, **G** is in alignment with selection in a substantial number of replicate runs, but out of alignment in other cases. The overall effect is for φ to vary in parallel with r_ω. Compared with a fixed mutational correlation, an evolving r_μ has pronounced effects on the variances and some other characteristics of the shape and size of the **G**-matrix (compare the corresponding rows in Table 1). For instance, with an evolving r_μ, the variances G_{ii}, the size Σ, and the leading eigenvalue λ_1 are nearly independent of r_ω, in contrast to the case when r_μ is held constant. In particular, for strong selectional correlation ($|r_\omega| \geq 0.75$), Σ is much larger with an evolving r_μ than with a constant (and small) r_μ. The second eigenvalues, λ_2, and ε are also much smaller in the cases of strong correlational selection so that the **G**-matrix is more eccentric, or cigar shaped.

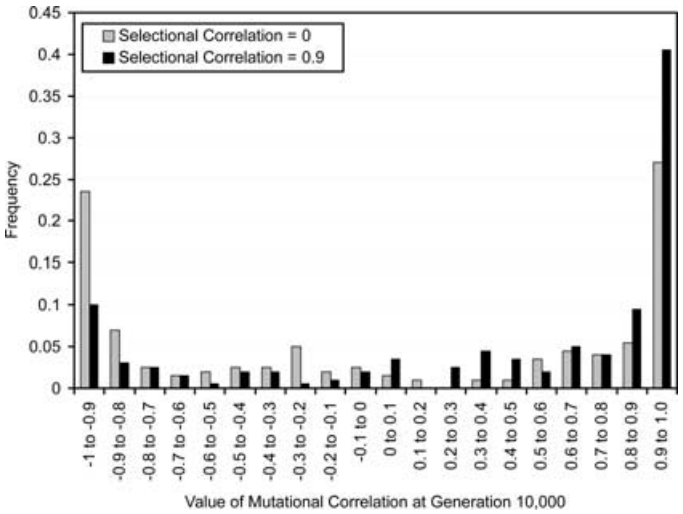

Figure 4. The distribution of mutational correlations at generation 10,000 for populations experiencing two different strengths of correlational selection. We used values of the selectional correlation of either 0 or 0.9. Other parameters are the same as in Table 2. Each histogram is based on 200 independent simulation runs, and the values of the mutational correlation are single-generation values obtained from the final generation of the simulation run (i.e., they are not means across generations or across runs).

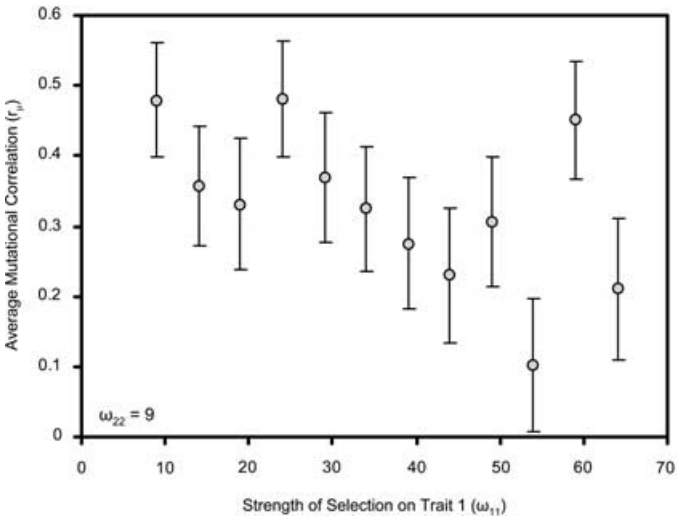

Figure 5. The evolution of the mutational correlation in response to variation in the angle of the adaptive landscape (i.e., the orientation of the ridge in two-trait space for a ridge-shaped individual selection surface). The value of ω_{22} was held constant at 9 and the value of ω_{11} varied from 9 to 64. As the ratio of ω_{11} to ω_{22} increases (from left to right), the angle of the adaptive landscape decreases. All other parameter values are equal to those described in Table 2. The decreasing values of the mutational correlation as the angle of the adaptive landscape decreases provide evidence that the mutational matrix evolves toward alignment with the adaptive landscape.

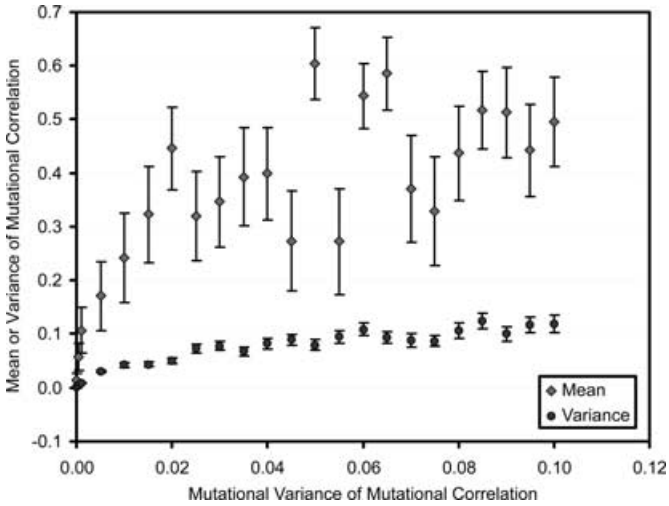

Figure 6. The influence of the mutational variance of the trait controlling the mutational correlation upon evolution of the mutational correlation. Each diamond shows a mean mutational correlation from 50 runs of the simulation, and error bars show one standard error. The circles indicate the average genetic variance of the mutational correlation. These simulations were performed using the same parameter values as in Table 2, except that we held r_ω constant at 0.90 and varied α_T^2 from 0.0001 to 0.5.

STABILITY OF THE G-MATRIX

Correlational selection has a stabilizing influence on both the mutational correlation and the **G**-matrix. Figures 9 and 10 show the dynamics of the mutational correlation and of the **G**-matrix during

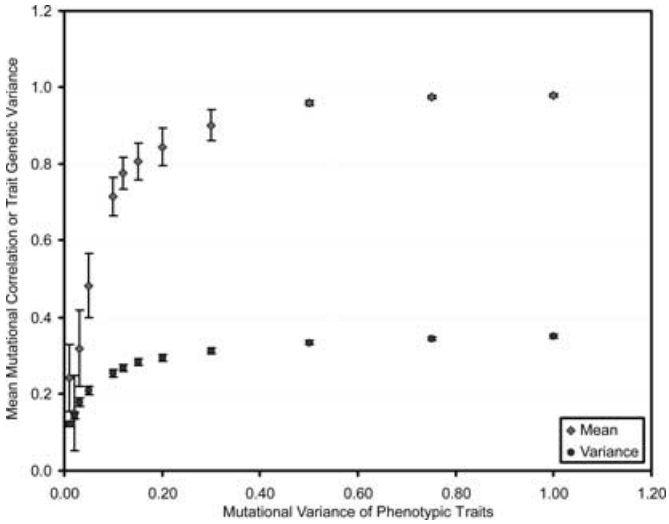

Figure 7. The effect of the mutational variances of the phenotypic traits on the evolution of the mutational correlation. Diamonds show mean mutational correlations across 50 replicate runs of the simulation, whereas circles show the mean additive genetic variance for the first phenotypic trait. Error bars show one standard error of the mean. Simulation parameters are identical to those listed in Table 2, except that we held r_ω constant at 0.90 and varied $\alpha_1^2 = \alpha_2^2$ from 0.01 to 1.0.

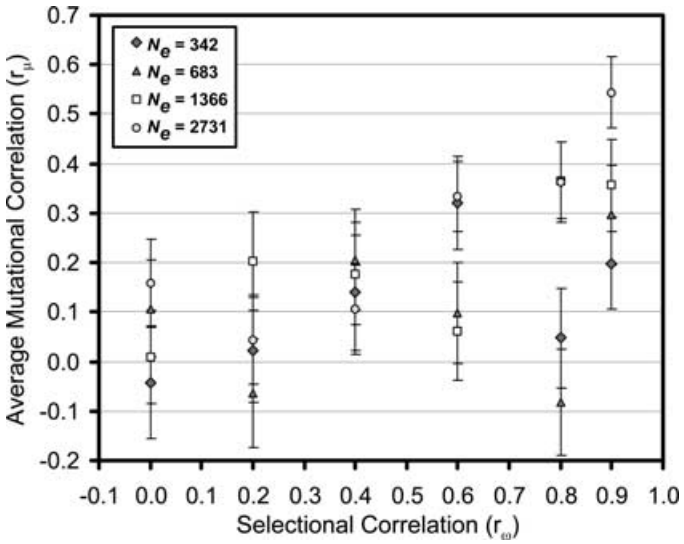

Figure 8. The evolution of the mutational correlation in populations of various sizes. These simulations used the standard parameter set (Table 2), except that we used four different population sizes, corresponding to effective sizes of 342, 683, 1366, and 2731. Means were calculated as described in Table 2 and error bars represent one standard error.

sample simulations with $r_\omega = 0$ and $r_\omega = 0.9$. In Figure 9, with $r_\omega = 0$, the mutational correlation drifts considerably, sometimes exhibiting positive and other times negative values. In Figure 10, with a selectional correlation of 0.9, the mutational correlation is almost always greater than zero. In other runs with $r_\omega > 0$ (not shown), the mutational correlation can be extremely negative at times, supporting the theoretical finding that disruptive selection acts on r_μ. Even in a large population, the **G**-matrix experiences episodes of instability arising from stochasticity in r_μ. Because of disruptive selection on r_μ, its evolution can swing between extreme values (i.e., near -1 to near $+1$), and these swings can promote instability of **G**. In general, as the mutational correlation drifts away from zero (top panel in Fig. 9), the angle of the **G**-matrix experiences periods of extreme stability (second panel from top) and becomes particularly eccentric, that is, ε becomes small (bottom panel). The angle, but also the eccentricity, is very unstable if the mutational correlation is close to zero (Fig. 9). Although the **G**-matrix remains extremely eccentric throughout the simulation run in Figure 10, it quickly loses some of its eccentricity when the mutational correlation dips down to zero near generation 2000. In each particular run, the evolution of the mutational

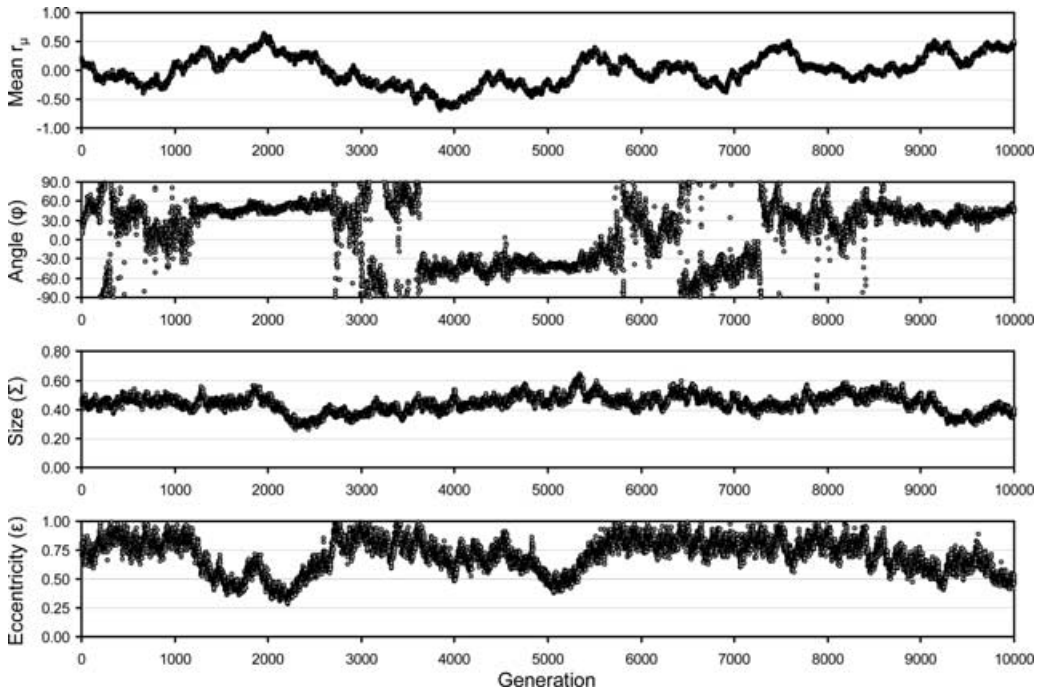

Figure 9. Dynamics of the mutational correlation, the angle of the G-matrix, the size of the G-matrix, and the eccentricity of the G-matrix during a sample run of the simulation with a selectional correlation of zero ($r_\omega = 0$). Each point of the graph plots the value of the variable of interest for a single generation. A simulation run of 10,000 generations is shown here. As the average mutational correlation drifts away from zero (top panel), the angle of the G-matrix experiences alternating periods of stability and instability (second panel from top). The evolution of the mutational correlation appears to have little effect on the size of the G-matrix (second panel from bottom). Other parameter values for this sample run are identical to those listed in Table 2.

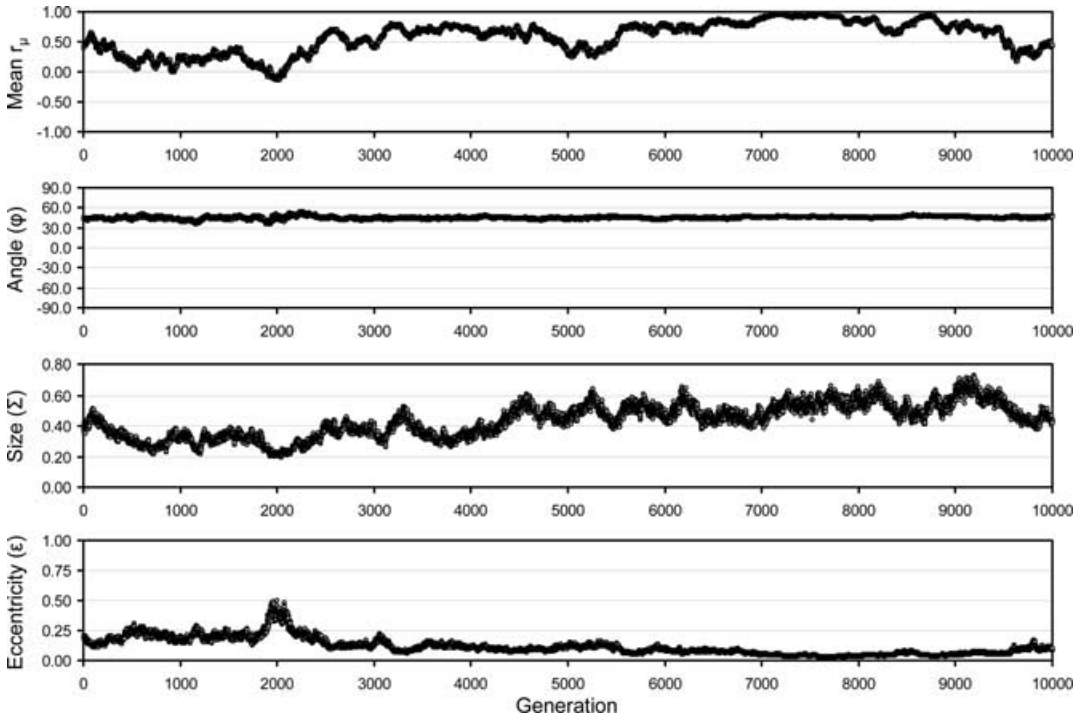

Figure 10. Dynamics of the mutational correlation, as well as the angle, sum, and eccentricity of G, during a sample simulation run with $r_\omega = 0.9$. Other parameter values are the same as those for Figure 9. Note that the mutational correlation drifts around, but tends to be greater than zero in this particular run (top panel). The angle of the G-matrix (second panel from top) is extremely stable, because it is stabilized by the nonzero mutational correlation and by the extremely strong correlational selection. The G-matrix remains extremely eccentric throughout this simulation run, but note that it quickly loses some of its eccentricity when the mutational correlation dips down close to zero near generation 2000.

correlation appears to have little effect on the size of the **G**-matrix (second panel from bottom). However, on average an evolving r_μ increases the size Σ if r_ω is nonzero (see above). The angle of the **G**-matrix (second panel from top) is extremely stable with large r_ω, because it is stabilized by the nonzero mutational correlation and by the extremely strong correlational selection, which cause the **G**-matrix to be cigar shaped and hence stable (Jones et al. 2003, 2004).

Perhaps the most remarkable effect of an evolving mutational correlation is its stabilization of the angle of the **G**-matrix. Figure 11 shows that an evolving mutational correlation results in a dramatic increase in stability of the **G**-matrix over most strengths of correlational selection. This increase is not so surprising when a nonevolving r_μ has the opposite sign of r_ω, but it is surprising that the stabilizing effect of an evolving r_μ is so large when r_ω is small, because then, on average, the evolving r_μ also is small (Table 1). This stabilization is produced by excursions of r_μ to relatively high positive and negative values that are sometimes long lasting (Fig. 9). The large stabilizing effect of nonzero values of the mutational correlation (Jones et al. 2003, 2004) and the tendency for the evolving mutational correlation to align with the

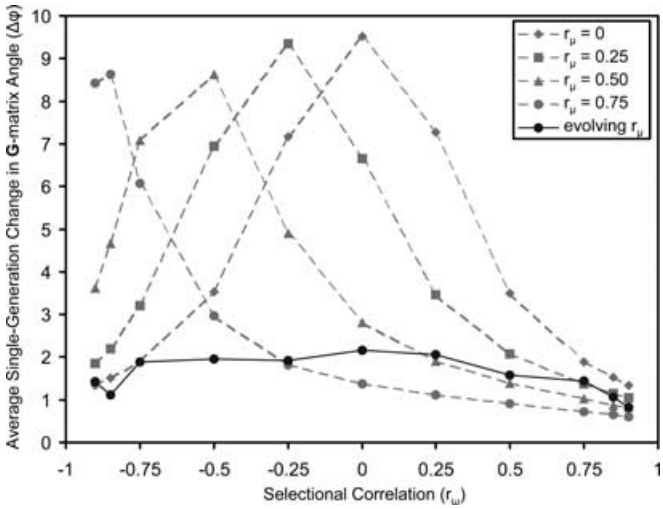

Figure 11. Stability of the angle of the G-matrix with fixed or evolving mutational correlations. The symbols connected by broken lines represent simulation runs in which the mutational correlations were held constant as a parameter in the simulation. The symbols connected by solid lines represent the situation in which the mutational correlation trait is allowed to evolve (see Table 2 for parameter values).

Table 3. The influence of the orientation of the adaptive landscape on the average per-generation change in the G-matrix when the mutational correlation is either evolving or fixed.

r_ω	r_μ	ΔG_{11}	ΔG_{22}	ΔG_{12}	Δr_g	$\Delta\lambda_1$	$\Delta\lambda_2$	$\Delta\Sigma$	$\Delta\varepsilon$	$\Delta\varphi$
Evolving r_μ										
−.90	−.30	.037	.037	.007	.012	.037	.040	.035	.055	1.4
−.75	−.12	.037	.037	.006	.014	.037	.039	.033	.053	1.9
−.50	.04	.037	.037	.006	.015	.037	.038	.032	.052	1.9
.00	.02	.037	.037	.006	.015	.037	.037	.032	.052	2.2
.50	.12	.037	.037	.006	.014	.037	.038	.032	.052	1.6
.75	.34	.037	.037	.007	.012	.037	.039	.034	.053	1.4
.90	.40	.037	.037	.007	.009	.037	.040	.035	.055	.8
Fixed r_μ										
−.90	.00	.038	.038	.004	.020	.038	.041	.031	.055	1.3
−.75	.00	.038	.038	.005	.022	.037	.039	.029	.053	1.9
−.50	.00	.038	.037	.005	.025	.037	.038	.028	.052	3.5
.00	.00	.037	.037	.006	.026	.037	.037	.027	.050	9.5
.50	.00	.038	.037	.005	.025	.037	.038	.028	.052	3.5
.75	.00	.038	.038	.005	.022	.037	.039	.029	.053	1.9
.90	.00	.038	.038	.004	.020	.038	.041	.031	.055	1.3
−.90	.50	.039	.039	.003	.026	.037	.043	.029	.055	3.6
−.75	.50	.038	.038	.003	.026	.037	.039	.028	.052	7.1
−.50	.50	.038	.038	.005	.026	.037	.037	.027	.051	8.6
.00	.50	.037	.037	.006	.024	.037	.037	.028	.052	2.8
.50	.50	.037	.037	.006	.020	.037	.037	.030	.052	1.4
.75	.50	.037	.038	.006	.017	.037	.038	.031	.052	1.0
.90	.50	.038	.038	.006	.014	.038	.039	.033	.053	.8

Note: These data are from the same simulation runs that were used to produce Table 2 (see Table 2 for parameter values). This table presents the mean single-generation change in each of the genetic variables (see text for details). The values of ΔG_{11}, ΔG_{22}, $\Delta\lambda_1$, $\Delta\lambda_2$, $\Delta\Sigma$, and $\Delta\varepsilon$ were standardized by dividing by their means (see Table 1), whereas ΔG_{12}, Δr_g, and $\Delta\varphi$ were not.

adaptive landscape contribute to this marked increase in stability. Of course, and as shown by Figure 11, if r_ω is positive and large, then a fixed, highly positive r_μ has a larger stabilizing effect on the angle than an evolving r_μ because it induces a pronounced and much more constantly cigar-shaped **G**-matrix.

As in our past work, some aspects of **G** stability are affected by population size and other aspects are affected by the curvature and orientation of the adaptive landscape (Jones et al. 2003, 2004). In contrast to its effects on the stability of the angle, an evolving r_μ has virtually no effect on the stability of the genetic variances, G_{ii}, and very little effect on the stability of the eigenvalues, the size, and the eccentricity (Table 3). Interestingly, for strong correlational selection, an evolving r_μ has a stabilizing effect on the genetic correlation, r_g, of the traits but a slightly destabilizing effect on their covariance (due to the higher genetic variances maintained under an evolving mutational correlation, Tables 2 and 3).

Discussion

Our results strengthen the growing realization that it is difficult, if not impossible, to draw a distinction between constraint and selection. The realization that the dichotomy is false recognizes the role that selection plays in shaping genetic constraints. As Schwenk and Wagner (2004) put it, "Constraints are forged in the fires of selection." Although the idea that selection shapes constraints has a long history in evolutionary biology, the arguments usually do not take the step of specifying how selection moulds constraint nor do they describe the pattern of those selective effects. In the theoretical literature, however, possible effects of selection on the **G**-matrix have been explicitly described for over 25 years (Lande 1980; Cheverud 1984; Jones et al. 2003, 2004). Those theoretical results indicate that multivariate stabilizing selection should have an especially important role in shaping the **G**-matrix. Although the **G**-matrix should experience stochastic fluctuation from generation to generation, particularly in small populations, as a long-term average, the **G**-matrix should represent a compromise between multivariate patterns imposed by selection on the one hand and mutation on the other. Thus, even if the process of mutation (e.g., embodied by the **M**-matrix) is a nonevolving constraint, the capacity of a population to evolve, as embodied by the **G**-matrix, is likely to bear the imprint of the population's selective history. The point of this article is to take

the argument further and ask whether the **M**-matrix might also reflect the history of multivariate stabilizing selection.

THE EVOLUTION OF MUTATIONAL CORRELATION

Stochasticity is a prominent result in our simulation study of the evolution of the **M**-matrix. This stochasticity could be expected from our analytical analysis of selection on the mutational correlation, a key aspect of the **M**-matrix, which showed that selection should be both weak and disruptive. Because of these selection aspects, we resorted to simulations in large populations ($N_e = 1366$) and on a relatively long time scale (10,000 generations) to capture trends in the evolution of the mutational correlation. The following general results emerged in these simulations. With relatively strong stabilizing selection ($\omega = 9$) imposed on each of two phenotypic traits in our runs, their phenotypic means drifted slightly about the optimum, never departing more than about 0.2 phenotypic standard deviations from the optimum. In contrast to this constrained stochasticity in phenotypic means, the mutational correlation often showed considerable fluctuation in value over the course of a simulation run, sometimes varying from nearly -0.9 to $+0.9$. Such stochastic fluctuation was markedly reduced when we imposed strong correlational selection (e.g., $r_\omega = 0.9$), corresponding to an adaptive landscape with a ridge-shaped hill with an orientation of 45° in phenotypic trait space. Under these conditions, the **M**-matrix evolved to an average position of alignment with the adaptive landscape in the majority of runs. Nevertheless, even under these conditions of strong selection, the average **M**-matrix was prone to large stochastic fluctuation. In general, the stronger the correlational selection, the higher the proportion of runs that showed alignment of **M** with the adaptive landscape. The tendency of **M** to evolve was also enhanced by genetic variance in the mutational correlation and by mutational variance in the two phenotypic traits experiencing stabilizing selection. Thus, our results support the view that pleiotropic mutation is not an invariant constraint but is instead susceptible to predictable evolution, albeit with superimposed randomness.

The present results suggest a program of research into the role of selection in shaping pleiotropic mutation. Aside from the obvious need for additional empirical studies of the **M**-matrix, we need companion estimates of multivariate stabilizing selection. A current and long standing weakness in empirical studies of phenotypic selection is the tendency to concentrate on the estimation of directional and stabilizing selection, while neglecting the study of correlational selection. Thus, in a recent comprehensive review of the selection literature (Kingsolver et al. 2001), there were too few estimates of correlational selection to permit a summary. Furthermore, the failure to treat the estimation of stabilizing selection as a multivariate problem means that most estimates of stabilizing selection may be biased (Turelli 1985). If we are to understand the evolution of the **M**-matrix, we will need parallel estimates of the γ-matrix (i.e., the matrix that describes the curvature of the adaptive landscape), including the off-diagonal elements that describe the strength of correlation selection, as well as the orientation of the adaptive landscape (Lande and Arnold 1983; Phillips and Arnold 1989; Arnold et al. 2001). Although we need such comparative work, the stochasticity evident in our simulations cautions that samples of **M**-matrices will be required to convincingly demonstrate trends produced by selection. Because of unstable evolutionary equilibria for elements of the **M**-matrix, any one estimate of the **M**-matrix may not be representative of historical influences of selection.

How can we reconcile our simulation results with the apparently contradictory predictions about selection on r_μ that arise from the Gaussian (eq. 9 and 10) and Zhang–Hill (eq. 13 and 14) expressions? Our results indicate that the simulated population is somewhere between these two cases. For example, the difference between the fitness minimum and maximum under the conditions depicted in Figure 2 is less than 0.001 under the Zhang–Hill theory but about 0.065 under the Gaussian theory. The empirical results from the simulation indicate a fitness differential of around 0.003. Thus, the simulated population is experiencing selection of a strength about three times greater than expected under the Zhang–Hill theory but still less than one-twentieth of what would be expected under the Gaussian model. Nevertheless, the simulation results clearly show evidence for disruptive selection on the mutational correlation (Figs. 2 and 4). In addition, the results in Figure 4 indicate a tendency for the mutational correlation to be positive when the selectional correlation is strongly positive, a result that is more in line with the predictions of the Gaussian model than those of the Zhang–Hill theory. However, consideration of weighted averages of the Gaussian and the Zhang–Hill predictions shows that giving only about 3% weight to the Gaussian produces a dependence of the mean fitness on r_μ very similar to that observed in Figure 2A. This result suggests that slight deviations from the Zhang–Hill scenario are sufficient to produce a dependence of fitness on r_μ that is very similar to the observed one. Regardless, the results indicate that the mutational correlation experiences weak disruptive selection that tends to produce convergence of the mutational and selectional correlations.

THE EVOLUTION OF THE G-MATRIX AND PHENOTYPIC INTEGRATION

Our results indicate that selection can directly and indirectly affect the evolution of the **G**-matrix. Curvature of the adaptive landscape and movement of the optimum can directly affect the evolution of **G** by promoting alignment of its eigenvectors with the principal axes of the adaptive landscape (Jones et al. 2003, 2004). The present results indicate that selection can also indirectly affect the evolution of **G** via effects on the **M**-matrix. In particular, our simulations show that alignment of the **M**-matrix with the adaptive

landscape is most likely to occur in large populations and on landscapes with steep slopes and axes with greatly differing eigenvalues (i.e., strengths of stabilizing selection). Even under these conditions, which are most favorable for alignment, the **M**-matrix is apparently prone to stochastic fluctuations that can produce long-term periods of misalignment or even antialignment. Thus, the way in which a population will respond to selection is directly affected by the evolution of the **G**-matrix and indirectly by the evolution of the **M**-matrix, both of which are shaped by selection.

Our results also help us understand the central observation of morphological integration: that functionally related traits tend to show significant phenotypic and genetic correlations (Olson and Miller 1958). It is easy to imagine that functionally coupled traits experience correlational selection (i.e., $\omega_{12} \neq 0$). Such selection favors particular combinations of character values. Thus, when two traits work together in a functional complex, it is to be expected that selection will favor trait values that match or otherwise work well in combination (Arnold 1988; Brodie 1992). Selection favoring tooth occlusion in mammals or a match between upper and lower culmen lengths in birds is a case in point. In our simulations we found that this mode of selection, in combination with large population size, helps to build genetic correlation by shaping the evolution of pleiotropic connections. However, the propensity for the mutational correlation to drift, even in large populations experiencing strong selection, suggests that instability of the **M**-matrix may be an intrinsic feature of genetic systems. For some suites of characters, however, functional or genetic constraints may dampen the random fluctuations in pleiotropic effects, so that **M** might be more stable than in our simulations. For other suites of characters, strong correlational selection on the traits may produce stability in the **G**-matrix, providing the illusion that the underlying mutational matrix also is stable. Furthermore, other factors, such as epistasis, could also be at work to prevent wholesale drift of mutational correlations, but additional empirical research on the genetic architecture of traits will be necessary before we can obtain a complete understanding of these phenomena.

THE MUTATIONAL MATRIX AND EVOLVABILITY

The evolution of the mutational matrix also enlightens our understanding of the evolution of evolvability. One major issue in the evolvability literature is simply the definition of evolvability. We favor the definition provided by Wagner and Altenberg (1996), which states, "Evolvability is the genome's ability to produce adaptive variants when acted upon by the genetic system." Consequently, the concept of evolvability embodies not only the nature of mutational variability in the population, but also the shape of the adaptive landscape. In the single-trait case, the concept of evolvability is thus relatively simple, as it must be related directly to the input of genetic variance due to mutation each generation. However, in multivariate phenotypic space, the concept of evolvability becomes much more complex and interesting.

In multivariate trait space, perhaps the most widespread concept of evolvability equates evolvability with modularity. In other words, evolvability is maximized when the mutational and genetic correlations for the traits in question are close to zero. If modularity is an important aspect of evolvability, then our results show that evolvability can evolve and respond to selection, because the evolutionary dynamics of the mutational correlation will change the evolvability of the population in question. However, our results also show that stabilizing selection favors decreased modularity, as the mutational correlation shows fitness maxima at $+1$ and -1. Thus, during periods of strong stabilizing selection, we expect populations to have a weak tendency to lose modularity if mutational correlations can evolve. Whether this expectation applies under directional selection will be the topic of future work.

Whereas modularity may be one useful concept related to evolvability, it may not always be the best way to capture the essence of evolvability. For example, Hansen (2003) shows that evolvability can profitably be viewed (in the two-trait case) as the ability of a character to respond to directional selection when the other character is under stabilizing selection. Hence, Hansen (2003) defines conditional evolvability as the conditional genetic variance matrix, which describes the short-term ability of a trait to respond to directional selection when other (potentially correlated) traits are constrained by selection. Interestingly, Hansen (2003) shows that minimization of pleiotropic effects does not necessarily produce the greatest conditional evolvability.

Our results suggest a different interpretation of evolvability, but resemble Hansen's (2003) in the sense that extreme modularity may not necessarily produce the greatest evolvability. In our models, the mutational matrix tends to align itself with the adaptive landscape. Alignment of the mutational matrix and the adaptive landscape also necessarily results in alignment of the **G**-matrix. Thus, populations will tend to evolve genetic lines of least resistance that are aligned with the ridge of the selection surface on a ridge-shaped adaptive landscape. Depending upon the model of peak movement, such alignment will have differing effects on evolvability. For example, certain suites of characters may have optima that predictably move along the ridge of the adaptive landscape (particularly if they are functionally integrated; Arnold et al. 2001). Such traits will tend to evolve strong mutational correlations, which will result in extremely high multivariate evolvability. On the other hand, some traits may have multivariate optima that move unpredictably with respect to the orientation of the adaptive landscape, and for those traits modularity would produce the greatest evolvability. Under our model, the disruptive selection on the mutational correlation would tend to decrease evolvability. Thus, our view is that the role of mutational correlations in

the evolution of evolvability depends critically on the model of peak movement.

THE STABILITY OF THE G-MATRIX

One of our most surprising results is that an evolving **M**-matrix tends to promote **G**-matrix stability. As in our past work, we found that stability in the angle of the **G**-matrix is promoted by those conditions that favor the evolution of a cigar-shaped (eccentric) **G**-matrix (e.g., correlational selection). In the present study, we found that an evolving mutational correlation promotes stability in the angle of the **G**-matrix, compared to the stability observed when the mutational correlation is not allowed to evolve. Nonevolving mutational correlations produce more **G**-matrix stability only when they are large and aligned with the adaptive landscape (Fig. 11).

The increase in stability that we observed for the **G**-matrix under an evolving mutational correlation was almost certainly due to the tendency for the mutational correlation to spend very little time near zero under any parameter combinations, coupled with the weak tendency for the mutational matrix to align itself with the adaptive landscape. The least favorable situations for **G**-matrix stability arise when the mutational correlation is near zero or when the mutational correlation is opposite in sign to the selectional correlation. Neither of these situations was likely to occur for prolonged periods in our simulations that allowed an evolving mutational correlation. The result is a surprisingly strong stabilization of the **G**-matrix in response to evolution of the mutational correlation.

LIMITATIONS OF THE MODEL AND FUTURE DIRECTIONS

Given the complexity of the issues, we were only able to explore a subset of the interesting aspects of mutational matrix evolution. Our results highlight many additional areas that would be worthy topics of future research. For the sake of simplicity, we dealt only with a landscape with a stationary optimum in the present study. Consequently, the population experienced mainly stabilizing selection, except during random excursions from the optimum, and most mutations were deleterious. Given our previous work on the evolution of the **G**-matrix (Jones et al. 2003, 2004), it is clear that most aspects of the evolution of the mutational correlation during stabilizing selection will apply during directional selection as well. However, there are certainly other aspects of **M**-matrix evolution that will only be revealed by additional work on a population evolving in response to a moving optimum. For example, our analytical theory implies that selection on the mutational correlation will be much stronger during directional selection than during stabilizing selection, so we may expect to see the effects of genetic drift diminish when the optimum is allowed to move.

One other characteristic of the present study is that we allow only the mutational correlation to evolve, while holding the diagonal elements of the **M**-matrix constant. The main reason to hold the mutational variances constant is that in the face of strong stabilizing selection, the mutational variances for the two traits would evolve toward zero, resulting in a population with no evolutionary potential whatsoever. Several theoretical studies of the evolution of mutational variances of single-traits clearly demonstrate such an effect, and the qualitative predictions of the theory apply to the evolution of the **M**-matrix for the multivariate phenotype. However, the quantitative evolutionary dynamics of an **M**-matrix in which all elements are capable of evolving in response to directional selection have not been investigated. A model of such an **M**-matrix would be quite complex, but also may yield interesting insights in to the evolution of genetic architecture and evolvability.

As with any theoretical study of quantitative genetic architecture, the model that we employed is not entirely biologically realistic. This situation arises from two main constraints. First, we simply do not possess enough empirical data regarding important genetic parameters to construct a perfectly realistic model. Second, limitations in theoretical analysis require certain simplifying assumptions. In our study we explore only a purely additive model of genotypic values, with an evolving mutational correlation, which is treated as a separate quantitative trait. The first major question is whether we should expect there to be a locus or a suite of loci that modify the mutational input at other quantitative traits. For some elements of the mutational matrix, such a scenario is certainly plausible. For example, the diagonal elements, which correspond to mutational variances, may depend on aspects of the genome that influence the rate at which mutations of large effect occur. The most obvious class of genes that could influence this process includes suppressors of transposable elements (McDonald 1995). Population-level variation at such loci could contribute to population-level variation in the mutational matrix. Variation at modifiers of mutational processes could plausibly produce variation among individuals in either mutational variances or covariances or both. Other classes of DNA elements that could contribute to mutational matrix evolution include trans-acting regulatory elements and highly mutable repetitive sequences (Schlötterer et al. 2006; Wratten et al. 2006). In addition, complex epistatic interactions could result in almost any conceivable effect on the mutational matrix (Hermisson et al. 2003). Thus, we expect the elements of the mutational matrix to exhibit some genetic variation. Two important but unresolved empirical questions are: (1) Do the elements of the mutational matrix respond to selection as if they have additive genetic variance? And, (2) how much genetic variance do these mutational traits exhibit in natural populations?

One important role of models of quantitative genetic phenomena, however, is to shine a spotlight on key but neglected genetic parameters. Although empirical studies (reviewed in Lande 1980)

reveal that pleiotropy is an almost universal property of genetic systems, only a few studies have documented the statistical properties of pleiotropic mutation (Lynch 1985; Houle et al. 1994; Fernández and López-Fanjul 1996; Camara and Pigliucci 1999; Keightley et al. 2000; Estes et al. 2005). These studies of mutational effect distributions often find mutational correlations of either zero, plus one or minus one. Intermediate values of mutational correlation are relatively uncommon (Lynch 1985; Houle et al. 1994; Fernández and López-Fanjul 1996; Camara and Pigliucci 1999; Keightley et al. 2000; Estes et al. 2005). In situations in which pleiotropy might be expected a priori on functional grounds, mutational correlations of plus or minus one are commonly found, suggesting that correlational selection has helped mold the pattern of pleiotropy. These observations are consistent with our theoretical and simulation results that reveal disruptive selection on mutational correlation. The question now is whether the empirical results are general, highlighting the need for additional work on pleiotropic mutation.

One robust pattern emerging from developmental biology and quantitative trait locus mapping is that epistasis is widespread and important. Thus, a more biologically accurate depiction of the evolution of the mutational matrix might be obtained through a fully realized model of epistasis, such as that described by Hermisson et al. (2003). Their multilinear model of epistasis permits mutational effects of existing alleles as well as the effects of new mutations to differ as a function the genetic background, thus allowing the **M**-matrix to evolve. Our model permits only a subset of these effects to occur and consequently can be seen as a sort of poor man's epistasis. Specifically, our model differs from the multilinear model of epistasis in that we do not permit the effects of existing alleles to change on different genetic backgrounds. However, our model shares the feature that the genetic background (embodied by the value of an individual's mutational correlation trait) affects the input of new mutation. Our model is sufficient to sketch the evolutionary pressures that drift and selection exert on the mutational correlation, but a more fully realized model of epistasis would no doubt lead to useful insights. We chose not to develop such a model as our first foray into the evolution of the **M**-matrix, because a complete model of epistasis, along the lines of Hermisson et al. (2003), would be vastly more complex than the model presented here and would involve literally hundreds of parameters. In addition, epistasis adds numerous complications to the interpretation of **G**-matrix evolution, as additive genetic variance is no longer easily separated from epistatic genetic variance. Nevertheless, the next logical step in the development of models of **M**-matrix evolution is to tackle these same issues with an explicit model of epistasis.

In light of the lack of empirical guidance for development of additional theory regarding **M**-matrix evolution, the next logical, but extremely daunting, empirical step would be to estimate genetic variances in the elements of the **M**-matrix. To what extent is the **M**-matrix capable of a response to selection? Genetic variation in mutational variance, covariance, and correlation has not been a target of empirical work. Estimating these varieties of genetic variation would be an extremely difficult experimental undertaking. Despite the difficulties of estimation, our results highlight the importance of genetic variation in mutational correlation, the genetic parameter that is crucial for response to selection. As noted above, genetic variation in r_μ probably arises from epistatic gene interactions. Thus, detection, if not estimation, of genetic variation in mutational correlation might be approached with selection experiments or quantitative trait locus studies of multiple traits.

One other simplification in the current study was the choice to restrict analysis to a phenotype comprising only two traits. Thus, **G** and **M** were simple two-by-two matrices. Even in the two-trait case, however, the issues are already quite complicated and the model has numerous parameters. A model involving a multivariate phenotype with greater than two traits requires the addition of numerous parameters. For example, in the three-trait case, the mutational matrix would have three off-diagonal elements representing each pair-wise mutational covariance. The manifestation of the mutational correlation that we used here would require each of these mutational correlations to be a distinct trait unless we assumed that mutational correlations among all pairs of traits were identical, which seems extremely unrealistic. Although an extension to multiple traits would be desirable on a number of grounds, we predict that most of the qualitative findings of the present study, as well as those of our previous studies of **G**-matrix stability (Jones et al. 2003, 2004), will also apply to phenotypes of three or more traits. Nevertheless, future work on phenotypes comprising numerous traits could be very enlightening with respect to the evolution of evolvability, as a more complex phenotype allows modularity to evolve in a much more interesting way than is possible in a two-trait system.

In summary, our analysis shows that the evolutionary dynamics of the mutational matrix, in particular the mutational correlation, are very interesting and have implications for the stability of the **G**-matrix and the capacity of a population to respond to selection. Hence, the evolutionary dynamics of the mutational matrix are central to an understanding of evolvability. Our exploratory study clearly shows that evolvability can respond to selection, and that the mutational matrix tends to align itself with the adaptive landscape. Additional theoretical and empirical work on this topic should lead to a better understanding of long-term evolutionary patterns.

ACKNOWLEDGMENTS

We are grateful to S. Estes for insightful discussion of this topic. This work was supported by the National Science Foundation (grant DEB-0447554 to SJA and RB and grant DEB-0448268 to AGJ).

LITERATURE CITED

Agrawal, A. F., E. D. Brodie III, and L. H. Rieseberg. 2001. Possible consequences of genes of major effect: transient changes in the G-matrix. Genetica 112–113:33–43.

Arnold, S. J. 1988. Quantitative genetics and selection in natural populations: microevolution of vertebral numbers in the garter snake *Thamnophis elegans*. Pp. 619–636 *in* B. S. Weir, E. J. Eisen, M. M. Goodman, and G. Namkoong, eds. Proceedings of the Second International Conference on Quantitative Genetics. Sinauer Associates, Sunderland, MA.

———. 1992. Constraints on phenotypic evolution. Am. Nat. 140:S85–S107.

Arnold, S. J., M. E. Pfrender, and A. G. Jones. 2001. The adaptive landscape as a conceptual bridge between micro- and macroevolution. Genetica 112/113:9–32.

Barton, N. H., and M. Turelli. 1989. Evolutionary quantitative genetics—how little do we know? Annu. Rev. Genet. 23:337–370.

Brodie, E. D., III. 1992. Correlational selection for color pattern and antipredator behavior in the garter snake *Thamnophis ordinoides*. Evolution 46:1284–1298.

Bürger, R. 2000. The mathematical theory of selection, recombination, and mutation. Wiley, Chichester, U.K.

Bürger, R., and R. Lande. 1994. On the distribution of the mean and variance of a quantitative trait under mutation-selection-drift balance. Genetics 138:901–912.

Bürger, R., G. P. Wagner, and F. Stettinger. 1989. How much heritable variation can be maintained in finite populations by mutation-selection balance. Evolution 43:1748–1766.

Camara, M., and M. Pigliucci. 1999. Mutational contribution to genetic variance-covariance matrices: an experimental approach using induced mutations in *Arabidopsis thaliana*. Evolution 53:1692–1703.

Cheverud, J. M. 1984. Quantitative genetics and developmental constraints on evolution by selection. J. Theor. Biol. 110:155–171.

———. 1996. Developmental integration and the evolution of pleiotropy. Am. Zool. 36:44–50.

Crow, J. F., and M. Kimura. 1964. The theory of genetic loads. Pp. 495–505 *in* S. J. Geerts, ed. Proceedings of the XI international congress of genetics. Pergamon, Oxford, U.K.

Dawkins, R. 1989. The evolution of evolvability. Pp. 201–220 *in* C. Langton, ed. Artificial life. Addison-Wesley, Santa Fe, NM.

Estes, S. R., B. C. Ajie, M. Lynch, and P. C. Phillips. 2005. Spontaneous mutational correlations for life history, morphological and behavioral characters in *Caenorhabditis elegans*. Genetics 170:645–653.

Fernández, J., and C. López-Fanjul. 1996. Spontaneous mutational variances and covariances for fitness-related traits in *Drosophila melanogaster*. Genetics 143:829–837.

Flury, B. 1988. Common principal components and related multivariate models. John Wiley and Sons, New York, NY.

Hansen, T. F. 2003. Is modularity necessary for evolvability? Remarks on the relationship between pleiotropy and evolvability. Biosystems 69:83–94.

Hansen, T. F., and D. Houle. 2004. Evolvability, stabilizing selection, and the problem of stasis. Pp. 130–150 *in* M. Pigliucci and K. Preston, eds. Phenotypic integration. Oxford Univ. Press, Oxford, UK.

Hermisson, J., T. F. Hansen, and G. P. Wagner. 2003. Epistasis in polygenic traits and the evolution of genetic architecture. Am. Nat. 161:708–734.

Houle, D., K. A. Hughes, D. K. Hoffmaster, J. Ihara, S. Assimocopoulous, D. Canada, and B. Charlesworth. 1994. The effects of spontaneous mutations on quantitative traits. I. Variances and covariances of life history traits. Genetics 138:773–785.

Jones, A. G., S. J. Arnold, and R. Bürger. 2003. Stability of the **G**-matrix in a population experiencing stabilizing selection, pleiotropic mutation, and genetic drift. Evolution 57:1747–1760.

Jones, A. G., S. J. Arnold, and R. Bürger. 2004. Evolution and stability of the **G**-matrix on a landscape with a moving optimum. Evolution 58:1639–1654.

Keightley, P. D., E. K. Davies, A. D. Peters, and R. G. Shaw. 2000. Properties of ethylmethane sulfonate-induced mutations affecting life history traits in *Caenorhabditis elegans* and inferences about bivariate distributions of mutation effects. Genetics 156:143–154.

Kingsolver, J. G., H. E. Hoekstra, J. M. Hoeskstra, D. Berrigan, S. N. Vignieri, C. E. Hill, A. Hoang, P. Gilbert, and P. Beerli, 2001. The strength of phenotypic selection in natural populations. Am. Nat. 157:245–261.

Kirschner, M., and J. Gerhart. 1998. Evolvability. Proc. Nat. Acad. Sci. U.S.A. 95:8420–8427.

Krall, C. 2005. Effects of pleiotropy on genetic variance and extinction time of small populations. [Ph.D. diss], Department of Mathematics, University of Vienna, Austria.

Lande, R. 1979. Quantitative genetic analysis of multivariate evolution, applied to brain: body size allometry. Evolution 33:402–416.

———. 1980. The genetic covariance between characters maintained by pleiotropic mutations. Genetics 94:203–215.

Lande, R., and S. J. Arnold. 1983. The measurement of selection on correlated characters. Evolution 37:1210–1226.

Liberman, U., and M. W. Feldman. 2005. On the evolution of epistasis I: diploids under selection. Theor. Popul. Biol. 67:141–160.

Lynch, M. 1985. Spontaneous mutation for life history characters in an obligate parthenogen. Evolution 39:804–818.

Lynch, M., and B. Walsh. 1998. Genetics and analysis of quantitative traits. Sinauer Associates, Sunderland, MA.

Lynch, M., M. Pfrender, K. Spitze, N. Lehman, J. Hicks, D. Allen, L. Latta, M. Ottene, F. Bogue, and J. Colbourne. 1999. The quantitative and molecular genetic architecture of a subdivided species. Evolution 53:100–110.

McDonald, J. F. 1995. Transposable elements—possible catalysts of organismic evolution. Trends Ecol. Evol. 10:123–126.

Olson, E. C., and R. I. Miller. 1958. Morphological Integration. Univ. Chicago Press, Chicago, IL.

Phillips, P. C., and S. J. Arnold, 1989. Visualizing multivariate selection. Evolution 43:1209–1222.

Radman, M., I. Matic, and F. Taddei. 1999. The evolution of evolvability. Ann. N. Y. Acad. Sci. 870:146–55.

Schlötterer, C., M. Imhof, H. Wang, V. Nolte, and B. Harr. 2006. Low abundance of Escherichia coli microsatellites is associated with an extremely low mutation rate. J. Evol. Biol. 19:1671–1676.

Schluter, D. 1996. Adaptive radiation along genetic lines of least resistance. Evolution 50:1766–1774.

Schwenk, K., and G. P. Wagner. 2004. The relativism of constraints on phenotypic evolution. Pp. 390–408 *in* M. Pigliucci and K. Preston, eds. Phenotypic integration: studying the ecology and evolution of complex phenotypes. Oxford Univ. Press, New York.

Turelli, M. 1984. Heritable genetic variation via mutation-selection balance: Lerch's zeta meets the abdominal bristle. Theor. Pop. Biol. 25:138–193.

———. 1985. Effects of pleiotropy on predictions concerning mutation-selection balance for polygenic traits. Genetics 111:165–195.

Wagner, G. P., and L. Altenberg. 1996. Complex adaptations and evolution of evolvability. Evolution 50:967–976.

Wratten, N. S., A. P. McGregor, P. J. Shaw, and G. A. Dover. 2006. Evolutionary and functional analysis of the *tailless* enhancer in *Musca domestica* and *Drosophila melanogaster*. Evol. Dev. 8:6–15.

Zhang, X. S., and W. G. Hill. 2002. Joint effects of pleiotropic selection and stabilizing selection on the maintenance of quantitative genetic variation at mutation-selection balance. Genetics 162:459–471.

Associate Editor: C. Goodnight